

Protein functional annotation of simultaneously improved stability, accuracy and false discovery rate achieved by a sequence-based deep learning

Jiajun Hong[†], Yongchao Luo[†], Yang Zhang, Junbiao Ying, Weiwei Xue, Tian Xie, Lin Tao and Feng Zhu 

Corresponding authors: Feng Zhu, College of Pharmaceutical Sciences, Zhejiang University, Hangzhou 310058, China. E-mail: zhufeng@zju.edu.cn; Lin Tao, School of Medicine, Hangzhou Normal University, Hangzhou 310036, China. E-mail: taolin@hznu.edu.cn

[†]These authors contributed equally to this work.

Abstract

Functional annotation of protein sequence with high accuracy has become one of the most important issues in modern biomedical studies, and computational approaches of significantly accelerated analysis process and enhanced accuracy are greatly desired. Although a variety of methods have been developed to elevate protein annotation accuracy, their ability in controlling false annotation rates remains either limited or not systematically evaluated. In this study, a protein encoding strategy, together with a deep learning algorithm, was proposed to control the false discovery rate in protein function annotation, and its performances were systematically compared with that of the traditional similarity-based and *de novo* approaches. Based on a comprehensive assessment from multiple perspectives, the proposed strategy and algorithm were found to perform better in both prediction stability and annotation accuracy compared with other *de novo* methods. Moreover, an in-depth assessment revealed that it possessed an improved capacity of controlling the false discovery rate compared with traditional methods. All in all, this study not only provided a comprehensive analysis on the performances of the newly proposed strategy but also provided a tool for the researcher in the fields of protein function annotation.

Key words: protein function prediction; deep learning; prediction stability; annotation accuracy; false discovery rate

Introduction

Functional annotation of protein sequence with high accuracy (AC) has become one of the most important issues in under-

standing the molecular mechanism of life [1, 2] and has great biological [3–5], pathological [6–8] and pharmaceutical [9–16] implications. With the rapid accumulation of a wealth of protein sequences, the functional annotation of proteins has become

Jiajun Hong, Yang Zhang and Junbiao Ying are doctoral, master's and undergraduate students at the College of Pharmaceutical Sciences in Zhejiang University, China, and jointly cultivated by the School of Pharmaceutical Sciences in Chongqing University, China. They are interested in artificial intelligence.

Weiwei Xue is a professor at the School of Pharmaceutical Sciences in Chongqing University, China. He is interested in the area of computer-based drug design and molecular dynamics simulation.

Tian Xie and Lin Tao are professors at the School of Medicine in Hangzhou Normal University, China. They are interested in the area of traditional Chinese medicine, bioinformatics and machine learning.

Feng Zhu is a professor at the College of Pharmaceutical Sciences in Zhejiang University, China. He got his PhD degree from the National University of Singapore, Singapore. His research group (<https://idrblab.org/>) has been working in the fields of bioinformatics, omics-based drug discovery, system biology and medicinal chemistry. Welcome to visit his personal website at: <https://idrblab.org/Peoples.php>.

Submitted: 6 May 2019; Received (in revised form): 27 May 2019

© The Author(s) 2019. Published by Oxford University Press.

This is an Open Access article distributed under the terms of the Creative Commons Attribution Non-Commercial License (<http://creativecommons.org/licenses/by-nc/4.0/>), which permits non-commercial re-use, distribution, and reproduction in any medium, provided the original work is properly cited.

For commercial re-use, please contact journals.permissions@oup.com

increasingly challenging [17]. Particularly, only ~1% of all protein sequences in UniProt [18] have experimentally verified functions [19–22], and it is estimated that ~90% of the annotated proteins in the ontology of molecular function (MF)/biological process (BP) [23] come from only nine species [24]. Even for these nine model organisms, ~60% of their proteins have not had any experimentally determined MF/BP term [24]. Traditional methods for protein function annotation are mainly based on the experiments such as mass spectrometry, microscopy and RNA interference, which are reported as very time-consuming and resource-demanding because of the low throughput and restricted scope of methodology [25–31]. As such, the computational approaches of significantly accelerated analysis process and enhanced AC are greatly desired [32–37].

Computational methods popular in current protein function prediction [38–40] can be roughly divided into three categories: information, structure and sequence based [41]. The information-based methods [26, 42–45] are suitable for predicting the functions of interacting proteins [46–49] and proteins from coexpressed genes [41, 47, 50] but seriously restricted by the great noises in protein–protein interaction data and insufficient number of annotated proteins [17, 41, 49]. The structure-based methods [51–54] are found to be accurate [47, 55] but significantly limited by the lack of crystallized protein folds or structures [47] and the unclear relations between structural similarity and functional similarity in many cases [41, 56]. Among those three method categories, the sequence-based ones have now become the most widely applied method in protein function prediction [41] due to the relatively easy access of abundant high-quality sequence data in public database [46, 50] and its powerful ability to predict the function of remotely relevant protein and the homologous proteins of distinct functions [47, 57]. There are two types of sequence-based approaches: similarity based and *de novo* [41]. Particularly, similarity-based methods (like BLAST (a tool used for finding regions of similarity between biological sequences) [58] and HMMER (a tool used for searching sequence databases for sequence homologs, and for making sequence alignments) [59]) assign an unannotated protein with the function of another protein similar in sequence to that protein [41]. Since the similarity-based methods are reported to depend heavily on the sequence homology, the *de novo* ones are considered as an effective complement [41, 60], which is irrespective of sequence similarity and good at predicting the distantly related proteins and the homologous proteins of distinct functions [61, 62]. The *de novo* methods are generally based on supervised learning model, such as K-nearest neighbor (KNN) [63], probabilistic neural network (PNN) [64] and support vector machine (SVM) [62]. They are reported to be powerful in predicting the functions of proteins [65–70] and other molecules [71].

However, the high false discovery rate of the sequence-based protein function prediction remains a severe problem [72–76]. In particular, the databases adopted by similarity-based methods for searching homology often contain noise, and the relation between sequence similarity and homology is sometimes unclear [41]; the representativeness of the training data analyzed by *de novo* method is not always sufficient [62]. In the past few years, several pioneer efforts have been made to solve the problems [77]. On one hand, a stringent score cutoff is adopted by BLAST and HMMER to control the false discovery hits in detecting homologies [78]. On the other hand, some machine learning methods have been used to identify false homologies [79, 80], and a putative negative training data set derived from representative seed proteins of Pfam families, which has high

coverage of the protein family space, is constructed to reduce the false discovery rate [62]. Recently, the deep learning algorithm is frequently applied in sequence and omics data analysis [81, 82], biomedical imaging and biomedical signal processing [83, 84], which demonstrates a remarkable performance [85]. In protein function annotation, a multitask deep neural network has been designed to predict the function of the proteins from multi-classes [83], and a deep restricted Boltzmann machine is used to annotate the proteins with Gene Ontology (GO) term in the deep position of a directed acyclic graph [23, 86]. Moreover, a multiclassification model has been constructed to predict protein functional classes [87]. Although those methods are reported to be effective in elevating protein annotation AC [88], their ability in controlling false annotation rates is either limited or not systematically evaluated [57]. Thus, the significant enhancement on controlling false discovery rate is still urgently needed, and the corresponding tool is required in the field of protein function annotation [62].

In this study, a protein encoding strategy, together with a deep learning algorithm, was proposed to control the false discovery rate in protein function annotation, and its performances were systematically compared to that of the traditional similarity-based and *de novo* methods. First, the training and testing data sets with the highest and lowest similarities were separately constructed for distinguishing the performances among different methods. Second, a protein encoding strategy was proposed and integrated to deep learning-based algorithm, and its performances were compared with other traditional methods from multiple perspectives. Third, the capacity of the proposed method in controlling the false discovery rate was assessed by the comprehensive genome scanning and enrichment factor (EF). In summary, this study provided a comprehensive analysis on the performances of a newly proposed protein function annotation strategy.

Materials and methods

The functional families studied in and protein sequences collected for this analysis

In total, 20 protein families of different GO terms were collected from diverse subclasses in the MF of the GO database by maximizing their representativeness among all MF categories [23], and the GO families with different numbers of proteins were selected to enable the discussion of the effect of sample size on prediction result. The total numbers of proteins in these GO families were from ~800 to ~33 500 (after removing repeated protein sequences). As provided in Table 1, each studied GO family was indicated by a GO ID [23], and the total number of proteins (with sequence length of ≤ 1000) in the 20 GO families were listed (ranging from 802 to 33 178). The sequences of the proteins in these 20 families were collected from the UniProt database [89], and the repeated sequences were removed to avoid possible bias.

Constructing the data sets of training and testing

Since a binary classification model was constructed for the studied GO families, the proteins in each family were considered as positive data. In order to significantly enhance the representativeness of negative data (nonmembers of a GO family), a putative data set was therefore constructed by considering the following steps: (1) the Pfam family of each protein in a particular GO family was collected from the Pfam database [90], (2) the Pfam families of all proteins in that GO family were considered as the

Table 1. Twenty GO families collected from diverse subclasses in MF of GO database by maximizing their representativeness among all MF categories. The numbers of proteins (with the sequence length of ≤ 1000) in these GO families were from 802 to 33 178, and the number of *Pfam* families covered by each GO family was from 57 to 1092. These GO families were sorted by their total numbers of proteins included

Functional GO families studied in this work	GO ID	No. of proteins	No. of <i>Pfam</i> families covered	No. of proteins in training data set	No. of proteins in testing data set
Cyclase activity	GO:0009975	802	57	624	178
Cyclin-dependent protein kinase activity	GO:0097472	2951	64	2295	656
Phosphoprotein phosphatase activity	GO:0004721	4324	152	3363	961
Transcription coregulator activity	GO:0003712	4684	346	3643	1041
Positive regulation of transferase activity	GO:0051347	4732	355	3680	1052
Negative regulation of catalytic activity	GO:0043086	6239	512	4853	1386
Transferase activity, transferring acyl groups	GO:0016746	8845	238	6879	1966
Ubiquitin-like protein transferase activity	GO:0019787	9553	255	7430	2123
Transferase activity, transferring glycosyl groups	GO:0016757	9694	278	7540	2154
Structural constituent of ribosome	GO:0003735	10 492	204	8160	2332
Regulation of hydrolase activity	GO:0051336	10 995	686	8551	2444
Positive regulation of catalytic activity	GO:0043085	11 803	719	9180	2623
Positive regulation of MF	GO:0044093	13 677	884	10 637	3040
Peptidase activity	GO:0008233	18 665	597	14 517	4148
DNA-binding transcription factor activity	GO:0003700	19 677	693	15 304	4373
Hydrolase activity, acting on ester bonds	GO:0016788	22 599	802	17 578	5021
Protein kinase activity	GO:0004672	23 068	642	17 942	5126
Hydrolase activity, acting on acid anhydrides	GO:0016817	28 327	779	22 032	6295
Signaling receptor activity	GO:0038023	28 700	525	22 322	6378
Catalytic complex	GO:1902494	33 178	1092	25 805	7373

‘positive *Pfam* family’ and (3) three representative seed proteins from the rest of the *Pfam* families (named as ‘negative *Pfam* family’) were collected to construct a putative negative data set (PND). Since the resulting PND was characterized by its proteins of significantly diverse *Pfam* families, its representativeness on those nonmembers of a GO family was substantially enhanced and could be applied for controlling false discovery [57, 62].

Moreover, the level of representativeness of the studied data sets has great impacts on the performances of the analyzed methods [62]. Particularly, the higher similarity between the data set used to construct models and that to test models could result in better functional prediction [57]. Thus, the training and testing data sets with the highest or the lowest similarity were constructed for the analyses here. First, the sequences were converted to digital vectors using the novel strategy proposed in this study (described in the following section). Second, the positive data set (containing all proteins from a particular GO family) was classified into six groups using the K-means clustering algorithm (the distance used in this clustering was Euclidean distance) [91]. On one hand, in order to construct the training and testing data sets with the highest similarity, one-third of proteins in each group of the positive data set were randomly selected out to construct the testing data set (combining six groups), and the remaining two-thirds were used to form training data set (combining six groups). On the other hand, to construct the training and testing data sets with the lowest similarity, two groups were randomly selected out from those six groups to construct the testing data set, and the remaining four were used to form training data set. For both situations, two out of those three representative seed proteins from the negative *Pfam* families were randomly selected out to form the training data set, and the remaining one was used to construct the testing data set. Furthermore, to evaluate the false discovery rate of those studied methods, all protein sequences in the human genome were collected from the UniProt database [89].

The methods studied and assessed in this work

The sequence homology was the basis of protein function prediction, which could be detected by similarity analysis among sequences. Generally, the sequences with higher similarity were more likely homologous. BLAST was one of the most popular tools for sequence similarity analysis [58]. Herein, the sequences of proteins in the training data set of each GO family were collected to construct a searchable database, and then any query protein was searched against this database using BLAST and annotated with the function of the most similar protein. HMMER was another popular tool for sequence similarity analysis used in this study, which was based on the hidden Markov model [59]. Similar to the BLAST, the searchable database was also constructed based on the sequences of proteins in the training data set of each GO family. Then, any protein was searched against this database using HMMER [59] and annotated based on the most similar one.

Moreover, there were three *de novo* methods studied and assessed in this study. The SVM tried to find a hyperplane to separate the members from nonmembers of a particular GO family by maximizing the margin defined in protein feature space [92]. The KNN predicted the class of a protein by the majority vote of its neighbors with a given distance metric [93], and the PNN was a neural network based on Bayesian decision theory [94]. These three methods were directly applied under the Python environment. As reported in the previous studies [57, 62], a method for converting the protein sequence to the digital feature vector had been successfully applied in SVM, KNN and PNN and had been shown good performance in protein function prediction. This method converted the protein sequence into the digital vector according to its properties and composition of amino acids [62, 95]. The properties adopted here included (1) hydrophobicity, (2) Van der Waals volume, (3) polarity, (4) polarizability, (5) charge, (6) secondary structure, (7) solvent accessibility and (8) surface tension [62, 96–98]. Each property was represented by three

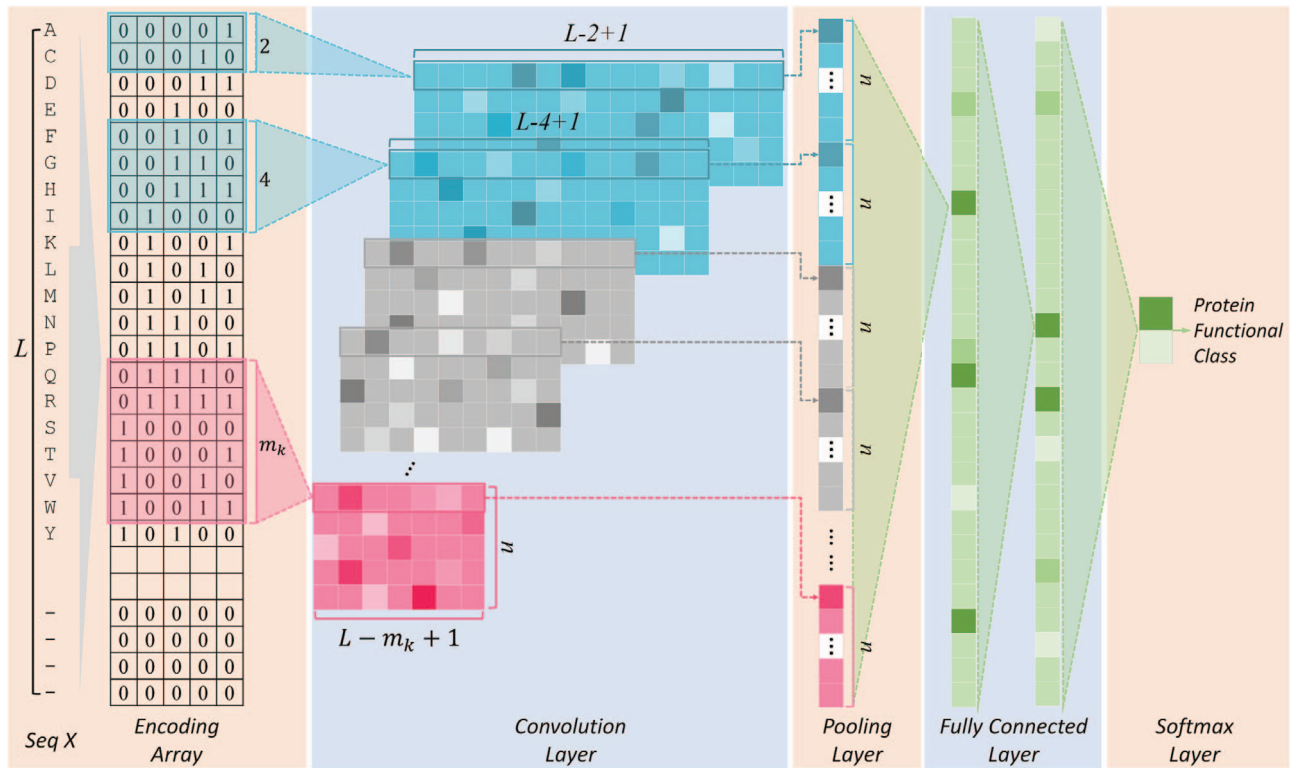


Figure 1. The workflow of the deep learning algorithm (CNN) applied together with the sequence encoding technique proposed in this study.

groups of descriptors: the global composition of given amino acid, frequencies with which the property changes along entire protein and distribution pattern of property along sequence. The detail on this digitalizing method could be found in previous studies [57, 62].

The deep learning algorithm used in this study was the convolutional neural network (CNN). As shown in Figure 1 (Encoding Layer), a new sequence encoding technique was first proposed to generate a 1000×5 binary array for any protein sequence. Particularly, each amino acid was encoded by a 5-bit binary number (from [0,0,0,0,1] for alanine to [1,0,1,0,0] for tyrosine). Only the proteins with the sequence length of no more than 1000 amino acids were analyzed in this study, which constitute the majority (>98%) of the proteins in any GO family. For the proteins of sequence length of less than 1000 amino acids, their empty amino acid positions were complemented by the 5-bit binary number [0,0,0,0,0]. Moreover, for the amino acids that were not among those 20 common ones, they were encoded by another number [1,0,1,0,1]. Second, CNN was applied, which consisted of multiple layers: a convolutional layer, a pooling layer, two fully connected layers and a softmax layer (Figure 1). The encoding array connected directly with the convolutional layer, which scanned the encoding array through an $m_k \times 5$ convolution kernel and resulted in a feature vector:

$$a_i^c = f \left(\sum_{j=1}^{m_k} \sum_{l=1}^5 (X_{(j+i-1)l} * W_{jl}) + b_i \right)$$

where a_i^c indicated the output of the i th neuron of the feature vector, m_k denoted the length of the k th convolution kernel, X referred to input protein encoding array and W and b_i were a $(m_k \times 5)$ weight array and a bias, respectively. f defined the ReLU

activation function [99]. Third, the max pooling layer was used, and the maximum neuron output value of the feature vector was selected as the output of the pooling layer.

$$a_j^{\max} = \max(a_i^c) \quad (i = 1, 2, \dots, L - m_k + 1)$$

where a_j^{\max} indicated the output of the j th neuron of the pooling layer. To fully extract protein features, eight different lengths of convolution kernel (for each length, there are 120 kernels) were used to scan the protein encoding array. Therefore, after the pooling layer, a vector containing 960 outputs for each protein was obtained. Fourth, using this vector, the fully connected layers generated the output for each layer:

$$a_i^{f1} = \sigma \left(\sum_{j=1}^{960} (a_j^{\max} * w_{ji}^{f1}) + b_i^{f1} \right)$$

$$a_j^{f2} = \sigma \left(\sum_{i=1}^{1000} (a_i^{f1} * w_{ji}^{f2}) + b_j^{f2} \right)$$

where a_i^{f1} denoted the output of the i th neuron of the first fully connected layer and a_j^{f2} referred to the output of the j th neuron of the second fully connected layer. w_{ji}^{f1} and b_i^{f1} indicated the j th weight and the bias of the i th neuron of the first fully connected layer; w_{ji}^{f2} and b_j^{f2} indicated the i th weight and the bias of the j th neuron of the second fully connected layer. σ was ELU activation function [100]. Finally, the output vector of the fully connected layer was further used as the input of a softmax layer, which provided the classification probability of the query protein:

$$Y = \text{softmax} (a^{f2} w' + b')$$

where a^{f2} indicated the output vector of the second fully connected layer and w' and b' referred to weight array and bias

Table 2. The performances of three *de novo* (SVM, KNN and PNN) and the deep learning (CNN) methods proposed in this study on the training and testing data sets (for eight representative GO families) with the highest similarity based on popular measurements (SE, SP, PR, AC and MCC). Each GO family was denoted by its GO ID, and its corresponding GO term was shown in Table 1

GO ID	CNN					SVM					KNN					PNN				
	SE%	SP%	PR%	AC%	MCC	SE%	SP%	PR%	AC%	MCC	SE%	SP%	PR%	AC%	MCC	SE%	SP%	PR%	AC%	MCC
GO:0097472	85.2	99.9	99.1	98.5	0.91	81.0	99.1	90.2	97.3	0.84	70.9	97.7	76.4	95.1	0.71	72.7	98.6	84.7	96.2	0.76
GO:0004721	79.5	99.2	93.9	96.6	0.85	65.2	99.3	93.2	94.7	0.75	68.0	95.6	70.8	91.9	0.65	55.5	98.7	87.0	92.9	0.66
GO:0051347	81.3	99.6	97.5	96.9	0.87	78.4	97.3	83.4	94.5	0.78	75.6	93.5	66.9	90.9	0.66	63.8	99.1	92.8	93.9	0.74
GO:0003735	80.7	98.7	95.8	93.8	0.84	87.2	97.6	93.2	94.8	0.87	84.7	95.6	87.8	92.6	0.81	84.9	95.5	87.7	92.6	0.81
GO:0016746	71.7	96.2	85.8	90.2	0.72	70.5	96.6	86.8	90.2	0.72	70.7	92.5	75.2	87.2	0.65	64.8	93.7	76.8	86.7	0.62
GO:0043085	69.3	98.1	94.3	89.2	0.74	75.4	95.2	87.5	89.1	0.74	78.8	87.1	73.2	84.5	0.65	66.7	95.6	87.2	86.7	0.68
GO:0003700	81.1	95.0	92.3	89.0	0.78	82.8	94.8	92.2	89.7	0.79	81.9	90.9	87.0	87.1	0.74	84.3	89.0	85.0	87.0	0.73
GO:0044093	80.7	93.5	86.6	89.1	0.76	78.7	94.1	87.5	88.8	0.75	80.6	85.5	74.5	83.8	0.65	72.6	92.5	83.7	85.6	0.68

vector, respectively. Y was the classification probability of sequence X (Figure 1).

The CNN model was implemented with the Python programming language and the TensorFlow library. The binary cross-entropy loss function was adopted in all models training, and the Adam [101] optimizer (learning rate = 0.001, $\beta_1 = 0.9$, $\beta_2 = 0.999$ and $\epsilon = 10^{-8}$) was used for the optimization during back-propagation. The weight parameters were initialized with the He initialization method [102], and biases were initialized to zero. The batch normalization was applied in the fully connected layers before ELU activation function for accelerating the speed of convergence, and the strategy of dropout [103] was also used in the fully connected layer with a drop rate of 0.6 to randomly remove a certain number of neurons at each training step in order to prevent the overfitting of the neural network.

Assessing the AC and false discovery rate of protein function annotation

Five popular measurements, such as sensitivity (SE), specificity (SP), precision (PR), AC and Matthews correlation coefficient (MCC) [57, 104], were adopted in this study to evaluate the performance of each protein functional annotation method. Since the SP was reported to be effective in evaluating the methods' false discovery rate [57], it was adopted in this study to assess the false discovery rate of the *de novo* methods and the constructed deep learning model based on the testing data set. Moreover, in order to further assess the false discovery rate of methods, a real-world application of the human genome scanning was performed with each method. For BLAST and HMMER, the training data set was used to construct the searching databases. For *de novo* and deep learning methods, the training data set was applied to train the models. Because it is not necessary to use the negative data set in predictions with BLAST and HMMER, the SP cannot be calculated in the genome scanning for both methods, the false discovery rate was evaluated by the EF for discovering the proteins in each GO family:

$$EF = \frac{(N_{PT}/N_P)}{(N_T/N)}$$

where N_P referred to the total number of proteins in the testing data set predicted by the method as the members of certain GO family, N_{PT} indicated the total number of predicted proteins in the testing data set truly belonging to this particular GO family, N denoted the total number of proteins in the studied genome and N_T referred to the total number of proteins in the testing data set truly belonging to the studied GO family. The value of

EF is no less than zero; however, only when the EF value is larger than 1, there is an enrichment. The larger the EF, the lower the false discovery rate.

Results and discussion

Methods' performances based on the training and testing data sets with the highest similarity

The performances of studied methods were first calculated and assessed based on the constructed training and testing data sets with the highest similarity (the way to construct such data sets was provided in the second section of Materials and Methods). As shown in Table 2, eight representative GO families were selected randomly from all 20 studied GO families, and the performances of three *de novo* (SVM, KNN and PNN) and the proposed deep learning (CNN) methods were provided based on five measurements (SE, SP, PR, AC and MCC). Taking AC as an example, it spanned from 89.0% to 98.5%, from 89.1% to 97.3%, from 84.5% to 95.1%, and from 86.7% to 96.2% for CNN, SVM, KNN and PNN, respectively. Moreover, for MCC, it ranged from 0.72 to 0.91, from 0.72 to 0.87, from 0.65 to 0.81, and from 0.62 to 0.81, respectively. As shown, the exact AC and MCC values of CNN and SVM were slightly higher than that of the remaining methods (KNN and PNN), but no significant difference was observed for AC values (the P-values for AC values between any two methods were larger than 0.05). For MCC values, CNN is better than KNN and PNN with the P-values of 0.004 and 0.011, respectively, SVM is better than KNN and PNN with the P-values of 0.012 and 0.038, respectively, and there is no significant difference between CNN and SVM.

The results above indicated that, for the data sets with the highest similarity, the studied methods showed a similar performance as each other. In other words, the models trained using the high representative data sets by difference methods performed consistently well, which denoted that the training and testing data sets with the highest similarity might have a low resolution on distinguishing the performances of different methods. Therefore, in order to provide an in-depth assessment on studied methods, the training and testing data sets with the lowest similarity could be considered as more effective in providing the performance assessment of higher resolution. Moreover, in the real world of protein function annotation, it was almost impossible to have all query proteins (with function unknown) fully represented by the proteins with annotated functions. Therefore, the assessment based on the data sets with the highest similarity could only draw the upper ceiling of the methods' performances, and the data sets in most real-world

Table 3. The performances of three *de novo* (SVM, KNN and PNN) and the deep learning (CNN) methods proposed in this study on the training and testing data sets (for 20 studied GO families) with the lowest similarity based on popular measurements (SE, SP, PR, AC and MCC). Each GO family was indicated by its GO ID, and its corresponding GO term was provided in Table 1

GO ID	CNN					SVM					KNN					PNN				
	SE%	SP%	PR%	AC%	MCC	SE%	SP%	PR%	AC%	MCC	SE%	SP%	PR%	AC%	MCC	SE%	SP%	PR%	AC%	MCC
GO:0009975	26.4	99.9	94.0	97.9	0.49	11.8	99.8	67.7	97.4	0.28	10.1	98.3	14.4	95.8	0.10	16.3	96.3	11.2	94.1	0.10
GO:0097472	67.7	99.9	99.6	96.9	0.81	39.0	99.3	85.1	93.5	0.55	43.3	97.8	67.6	92.6	0.50	40.2	98.6	74.8	93.0	0.52
GO:0004721	55.6	99.5	94.5	93.6	0.70	28.4	99.2	84.0	89.7	0.45	36.4	95.2	54.2	87.3	0.38	32.4	97.3	64.8	88.5	0.40
GO:0003712	32.7	99.7	94.2	89.9	0.52	20.4	98.5	70.2	87.1	0.33	35.9	94.5	52.5	85.9	0.36	38.1	92.9	47.8	84.9	0.34
GO:0051347	42.5	99.9	98.7	91.4	0.62	26.9	98.8	79.3	88.2	0.42	37.4	92.7	47.0	84.5	0.33	37.5	96.0	62.0	87.4	0.42
GO:0043086	35.5	99.1	90.4	87.1	0.52	17.4	98.0	66.4	82.8	0.28	28.7	91.8	44.8	79.9	0.25	10.1	99.9	96.6	83.0	0.28
GO:0016746	40.0	97.7	84.9	83.7	0.51	27.1	93.7	58.0	77.5	0.28	30.0	86.2	41.1	72.5	0.18	9.9	99.4	84.8	77.7	0.24
GO:0019787	79.9	96.2	87.8	92.0	0.79	37.7	96.1	76.9	81.1	0.44	34.8	90.3	55.4	76.0	0.30	40.1	89.9	57.9	77.1	0.34
GO:0016757	48.9	97.3	86.5	84.7	0.57	22.0	96.2	68.0	77.0	0.29	38.5	84.9	47.2	72.8	0.25	32.7	92.7	61.2	77.1	0.32
GO:0003735	87.6	97.3	92.4	94.6	0.86	87.9	96.6	90.8	94.2	0.85	86.0	95.0	86.7	92.6	0.81	84.4	93.1	82.2	90.7	0.77
GO:0051336	28.3	98.9	91.2	78.2	0.43	23.0	94.4	63.1	73.5	0.26	38.6	84.3	50.5	70.9	0.25	46.5	83.2	53.4	72.4	0.31
GO:0043085	44.0	98.0	90.7	81.3	0.54	32.9	94.9	74.3	75.7	0.37	54.8	79.8	54.9	72.1	0.35	57.8	80.5	57.0	73.5	0.38
GO:0044093	41.6	96.3	85.4	77.5	0.48	29.0	94.6	73.9	72.0	0.33	46.7	80.2	55.4	68.7	0.28	23.1	97.3	81.7	71.7	0.33
GO:0008233	62.0	92.9	86.0	80.2	0.59	49.2	92.8	82.7	74.9	0.48	67.9	72.6	63.4	70.7	0.40	60.6	80.7	68.7	72.4	0.42
GO:0003700	77.7	94.1	90.7	87.1	0.74	62.2	89.1	81.0	77.6	0.54	67.0	85.2	77.1	77.4	0.53	68.2	84.5	76.6	77.5	0.54
GO:0016788	53.9	89.1	81.0	72.8	0.46	45.9	86.5	74.5	67.6	0.36	64.8	65.0	61.5	64.9	0.30	55.9	78.2	68.9	67.8	0.35
GO:0004672	76.8	95.5	93.7	86.8	0.74	49.1	88.0	78.1	69.9	0.41	60.3	71.7	65.0	66.4	0.32	50.9	86.6	76.8	70.0	0.40
GO:0016817	60.7	95.0	92.9	77.1	0.59	45.3	84.9	76.5	64.3	0.33	68.2	60.8	65.4	64.7	0.29	67.1	65.4	67.8	66.3	0.32
GO:0038023	71.3	91.6	90.0	81.1	0.64	59.4	90.6	87.1	74.5	0.52	57.2	83.7	78.9	70.0	0.42	57.0	84.7	79.9	70.4	0.43
GO:1902494	49.6	87.2	83.4	66.0	0.39	42.8	79.9	73.4	59.0	0.24	58.6	62.5	66.9	60.3	0.21	58.9	66.6	69.6	62.3	0.25

occasions were much less representative. Especially for the novel or newly discovered proteins, which attract great and broad attentions, the training data set or database could not provide any representativeness to the novel ones. Therefore, compared with the upper ceiling, a bottom line (the training and testing data sets with the lowest similarity) was expected to be capable of revealing the lower limits of the performances of all studied methods.

Methods' performances based on the training and testing data sets with the lowest similarity

The performances of the studied methods were calculated and assessed based on the constructed data sets with the lowest similarity (the way to construct such data sets was provided in the second section of Materials and Methods). As illustrated in Table 3, the performances of three *de novo* and one deep learning methods on all 20 GO families were provided based on five measurements. Moreover, the statistical differences of these measurements between any two methods were shown in Figure 2. As one of the most comprehensive parameters in any category of predictors [57], the MCC reflected the stability of protein function predictor, which described the correlation between a predictive value and the actual value [62, 105, 106]. As illustrated on the left panel of Figure 2A, the variations of MCC values among methods were provided (the actual MCC value of each method was subtracted by the minimum MCC value among four different methods). As shown, the CNN method showed the consistently higher MCC values compared with the other three methods, and the MCC values of KNN method were the lowest in most of the GO families. As all GO families were ordered by their total numbers of proteins, there was no clear trend on the MCC values with the increase of protein amount. Moreover, to assess the statistical differences of MCC values between any two methods, the violin box plots based on the MCC values in Table 3 were drawn on the right panel of Figure 2A. As illustrated,

there were significant differences ($P < 0.01$) between the MCCs of CNN and that of the rest methods, and there was no significant difference in MCCs between any two of those three *de novo* methods. These results demonstrated an enhanced stability of the CNN-based protein function annotation model compared with three popular *de novo* methods.

As another important parameter for protein function annotation assessment, the AC referred to the total number of true members (positive plus negative) divided by the number of studied proteins [57], which was essential to be compared among different methods. Herein, the variations of AC values among methods (the actual AC of each method was subtracted by the minimum ACs among four different methods) were therefore calculated and provided on the left panel of Figure 2B. Similar to MCCs, the CNN method showed the consistently higher AC values compared with other three methods, and the AC values of KNN method were also the lowest in most of those GO families (there was no clear trend on the AC values with the increase of protein amount either). Furthermore, to assess the statistical differences of the ACs between any two methods, the violin box plot based on the ACs in Table 3 was drawn on the right panel of Figure 2B. As illustrated, there were significant differences ($P < 0.05$) between the AC values of CNN and that of the rest methods, and there was no significant difference in ACs between any two of those three *de novo* methods. These results showed the elevated AC of the CNN-based protein function annotation model compared with three popular *de novo* methods.

Besides the stability (MCC) and AC, SE and SP were also frequently used to assess the methods' prediction performances on positive and negative data sets, respectively. Thus, in this study, similar analyses were also conducted and shown in Figure 2C, D. Since the SP was known as an effective metric reflecting the false discovery rate, both CNN and SVM showed enhanced control on the false discovery when comparing with KNN and PNN. All in all, based on the comprehensive assessment from four different perspectives (MCC, AC, SE and SP), the CNN method

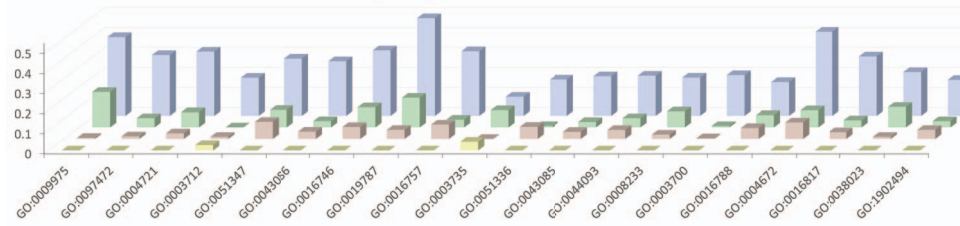
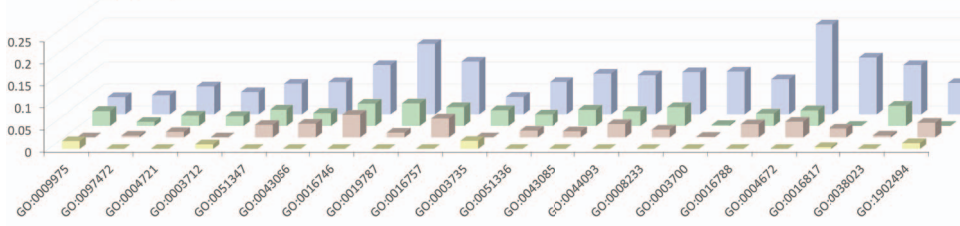
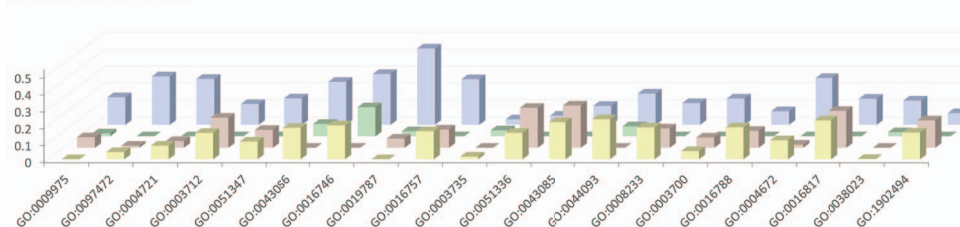
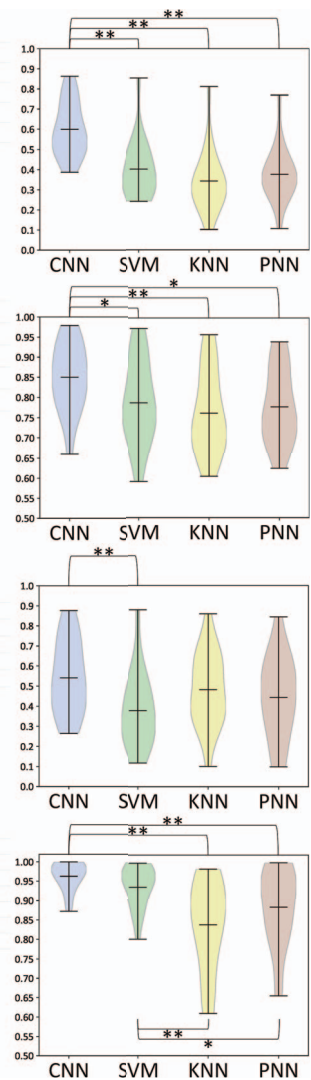
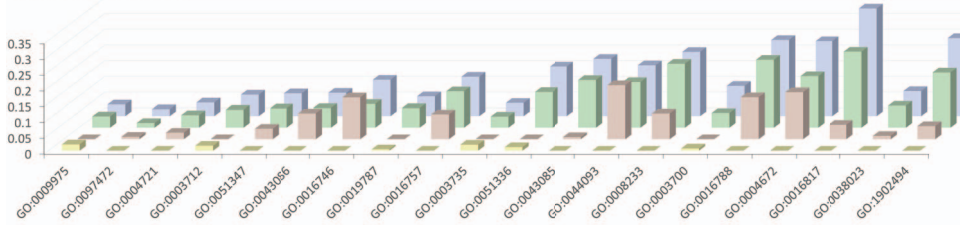
A: Matthews Correlation Coefficient (MCC)**B: Accuracy (ACC)****C: Sensitivity (SEN)****D: Specificity (SPE)**

Figure 2. Variations (the actual value of each method subtracted by the minimum value among four different methods) of four measurements among different protein function annotation methods: (A) MCC, (B) AC, (C) SE, (D) SP. On the right side, the statistical differences between any two methods were provided as the violin box plots. * indicated great difference of $P < 0.05$, and ** denoted significant difference of $P < 0.01$. Detailed P-values are provided in [Supplementary Table S1](#).

proposed here was found to perform better in both prediction stability and annotation AC compared with three popular *de novo* methods. Although both CNN and SVM were found with enhanced control of false discovery rate, the SEs of CNN were found to be significantly enhanced ($P=0.007$) compared with that of SVM.

In-depth assessment on the false discovery rates based on genome scanning

Besides the SP, the EF was one of the most popular and effective metrics for assessing the false discovery rate of any functional annotation method [57]. As known, the SP values assess the false discovery rate via only considering the prediction performance on the PND, while the EF evaluates the false discovery by fully considering the real-world true members of a particular GO family. Therefore, the EFs were applied in this study to complement the SP and further make in-depth assessment on the false discovery rate of each studied methods. In other words, in order to evaluate the false discovery rate of each method in the real

world, multiple methods (CNN, BLAST, HMMER, SVM, KNN and PNN) were used to scan the human genome to identify human proteins belonging to each GO family. As shown in [Table 4](#), the total numbers of proteins identified by different methods together with their corresponding EFs were provided. Moreover, the EFs of each method based on different GO families were illustrated in [Figure 3](#). As shown, there were clear variations among the EFs of different methods. Particularly, as shown on the right panel of [Figure 3](#), there were significant differences ($P < 0.01$) between the EFs of CNN and that of all *de novo* methods and BLAST. Based on the statistical analysis conducted in this study, there was no significant variation between the EFs of CNN and that of PHMM (a probabilistic model called Poisson Hidden Markov Model, which used in the HMMER), but the calculated P-value (0.054) was very close to 0.05. Furthermore, as provided in [Table 4](#), the majority (17 out of 20, 85.0%) of the EFs of CNN were higher than that of PHMM. In conclusion, based on the information provided in [Figure 3](#) and [Table 4](#), the deep learning strategy CNN proposed in this study showed an improved ability to control the false discovery rate.

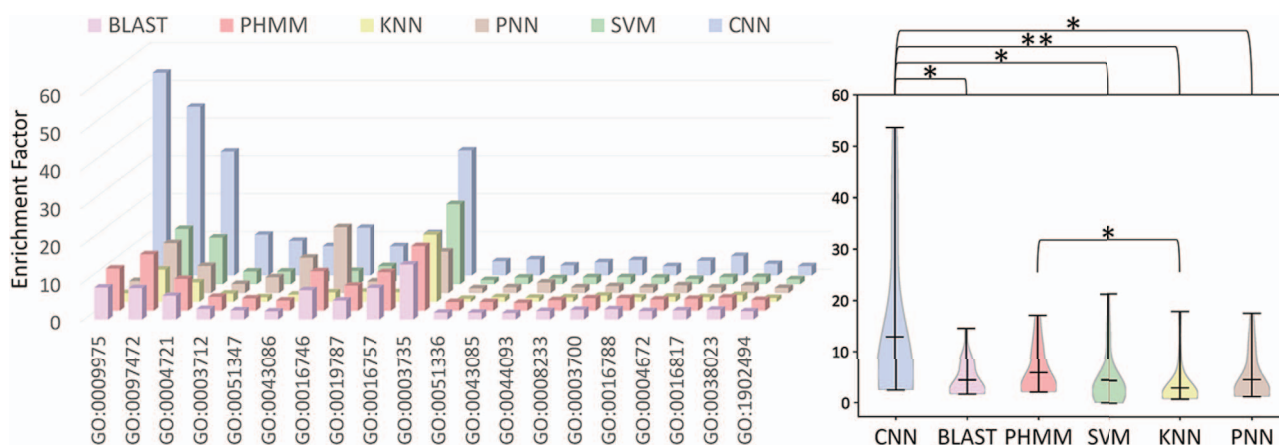


Figure 3. The EFs of different protein function annotation methods of the training and testing data sets (for all studied GO families) with the lowest similarity. On the right side, the statistical differences of the EFs between any two methods were provided as the violin box plots. * indicated great difference of $P < 0.05$, and ** denoted significant difference of $P < 0.01$. Detailed P-values are provided in the [Supplementary Table S2](#).

Table 4. The total numbers of proteins and the EFs of three *de novo* (SVM, KNN and PNN) identified by two similarity-based (BLAST and HMMER) and the deep learning (CNN) methods proposed in this study based on the training and testing data sets (for all 20 studied GO families) of the lowest similarity. Each GO family was indicated by its GO ID, and its corresponding GO term was provided in [Table 1](#)

GO ID	No. of proteins identified by each method						EF					
	CNN	SVM	KNN	PNN	BLAST	PHMM	CNN	SVM	KNN	PNN	BLAST	PHMM
GO:0009975	56	235	657	1416	1594	1347	53.61	0	2.28	3.18	8.48	11.14
GO:0097472	202	434	619	561	1598	923	44.59	14.65	8.56	13.22	8.29	14.92
GO:0004721	352	712	1824	1402	2403	1844	32.73	12.36	5.17	7.17	6.28	8.41
GO:0003712	637	1403	2648	3114	4408	3541	10.79	3.38	2.19	2.40	2.80	3.65
GO:0051347	725	1689	3873	1421	5858	4521	9.15	3.37	1.22	4.17	2.43	3.22
GO:0043086	1087	2291	3822	528	5911	4888	7.75	2.63	1.92	9.37	2.14	2.67
GO:0016746	924	2173	3878	401	2076	1604	12.61	3.51	2.51	17.44	7.76	10.44
GO:0019787	1954	2339	3822	3921	3328	2499	7.72	4.79	2.67	3.06	5.02	6.62
GO:0016757	881	1265	4146	2352	1770	1451	11.20	6.05	2.56	3.88	8.36	10.20
GO:0003735	520	750	965	1564	1207	1029	33.03	21.22	17.8	10.98	14.58	17.10
GO:0051336	1436	4334	6885	6693	7187	5887	3.76	1.10	0.81	1.26	1.81	2.28
GO:0043085	2152	4710	8846	8082	7984	6470	4.27	1.78	1.23	1.53	1.83	2.29
GO:0044093	3458	5172	9417	2664	8654	7048	2.65	1.61	1.10	2.79	1.69	2.07
GO:0008233	2850	3842	8106	5906	5409	4327	3.52	1.85	1.18	1.50	2.24	2.77
GO:0003700	3877	6586	6861	6604	6537	5167	4.07	1.87	1.66	1.84	2.58	3.27
GO:0016788	3975	4867	9351	7019	5338	4414	2.45	1.75	1.18	1.52	2.72	3.33
GO:0004672	2904	5918	8287	4895	6621	4633	3.87	1.40	1.35	2.05	2.21	2.96
GO:0016817	2207	5443	10 649	8903	6531	5053	5.15	1.89	1.24	1.48	2.43	3.13
GO:0038023	4230	5919	7314	6684	5616	3573	3.06	1.93	1.79	2.03	2.60	3.48
GO:1902494	4133	6900	10 017	8399	6466	4991	2.45	1.31	1.04	1.35	2.16	2.84

Conclusions

Based on the comprehensive assessment using different measurements (MCC, AC, SE and SP), the CNN method together with the protein encoding strategy proposed in this study was found to perform better in both prediction stability and annotation AC compared with the popular *de novo* methods. Moreover, the in-depth assessment revealed that it possessed an improved capacity of controlling the false discovery rate in current protein functional annotation compared with other traditional methods. All in all, this study not only provided a comprehensive analysis on the performances of the newly proposed strategy but also provided a valuable tool for the researcher in the fields of protein function annotation.

Key Points

- Functional annotation of protein sequence with high accuracy has become one of the most important issues in modern biomedical studies.
- A protein encoding strategy, together with a deep learning algorithm, was proposed to control false discovery rate in protein function annotation.
- The proposed strategy and algorithm were found to perform better in prediction stability, annotation accuracy and false discovery rate compared with the traditional methods.

Supplementary Data

Supplementary data are available online at <https://academic.oup.com/bib>.

Acknowledgments

This study was funded by the National Key Research and Development Program of China (2018YFC0910500), National Natural Science Foundation of China (81872798), Fundamental Research Funds for Central Universities (2018QNA7023, 10611CDJXZ238826, 2018CDQYSG0007 and CDJZR14468801), Innovation Project on Industrial Generic Key Technologies of Chongqing (cstc2015zdcy-ztxx120003), Key Project of Zhejiang Province Ministry of Science and Technology (2015C03055) and Key Project of National Natural Science Foundation of China (81730108).

References

- Chang YC, Hu Z, Rachlin J, et al. COMBEX-DB: an experiment centered database of protein function: knowledge, predictions and knowledge gaps. *Nucleic Acids Res* 2016;**44**:D330–5.
- Sahraeian SM, Luo KR, Brenner SE. SIFTER search: a web server for accurate phylogeny-based protein function prediction. *Nucleic Acids Res* 2015;**43**:W141–7.
- Goldstrohm AC, Hall TMT, McKenney KM. Post-transcriptional regulatory functions of mammalian Pumilio proteins. *Trends Genet* 2018;**34**:972–90.
- Qiao W, Akhter N, Fang X, et al. From mutations to mechanisms and dysfunction via computation and mining of protein energy landscapes. *BMC Genomics* 2018;**19**:671.
- Woods RJ. Predicting the structures of glycans, glycoproteins, and their complexes. *Chem Rev* 2018;**118**:8005–24.
- Shiihashi G, Ito D, Yagi T, et al. Mislocated FUS is sufficient for gain-of-toxic-function amyotrophic lateral sclerosis phenotypes in mice. *Brain* 2016;**139**:2380–94.
- Skrlić B, Konc J, Kunej T. Identification of sequence variants within experimentally validated protein interaction sites provides new insights into molecular mechanisms of disease development. *Mol Inform* 2017;**36**:00017.
- Seneviratne U, Nott A, Bhat VB, et al. S-nitrosation of proteins relevant to Alzheimer's disease during early stages of neurodegeneration. *Proc Natl Acad Sci U S A* 2016;**113**:4152–7.
- Li B, Tang J, Yang Q, et al. NOREVA: normalization and evaluation of MS-based metabolomics data. *Nucleic Acids Res* 2017;**45**:W162–70.
- Li B, Tang J, Yang Q, et al. Performance evaluation and online realization of data-driven normalization methods used in LC/MS based untargeted metabolomics analysis. *Sci Rep* 2016;**6**:38881.
- Lai AC, Crews CM. Induced protein degradation: an emerging drug discovery paradigm. *Nat Rev Drug Discov* 2017;**16**:101–14.
- Tang J, Fu J, Wang Y, et al. Simultaneous improvement in the precision, accuracy and robustness of label-free proteome quantification by optimizing data manipulation chains. *Mol Cell Proteomics* 2019; doi:10.1074/mcp.RA118.001169.
- Li YH, Li XX, Hong JJ, et al. Clinical trials, progression-speed differentiating features and swiftness rule of the innovative targets of first-in-class drugs. *Brief Bioinform* 2019; doi:10.1093/bib/bby130.
- Zhang Y, Ying JB, Hong JJ, et al. How does chirality determine the selective inhibition of histone deacetylase 6? A lesson from trichostatin a enantiomers based on molecular dynamics. *ACS Chem Neurosci* 2019;**10**:2467–80.
- Li X, Li X, Li Y, et al. What makes species productive of anti-cancer drugs? Clues from drugs' species origin, drug-likeness, target and pathway. *Anticancer Agents Med Chem* 2018;**19**:194–203.
- Han Z, Xue W, Tao L, et al. Identification of key long non-coding RNAs in the pathology of Alzheimer's disease and their functions based on genome-wide associations study, microarray, and RNA-seq data. *J Alzheimers Dis* 2019;**68**:339–55.
- Zhao B, Hu S, Li X, et al. An efficient method for protein function annotation based on multilayer protein networks. *Hum Genomics* 2016;**10**:33.
- The UniProt Consortium. UniProt: the universal protein knowledgebase. *Nucleic Acids Res* 2017;**45**:D158–69.
- Das S, Orengo CA. Protein function annotation using protein domain family resources. *Methods* 2016;**93**:24–34.
- You R, Zhang Z, Xiong Y, et al. GOLabeler: improving sequence-based large-scale protein function prediction by learning to rank. *Bioinformatics* 2018;**34**:2465–73.
- Tang J, Fu J, Wang Y, et al. ANPELA: analysis and performance assessment of the label-free quantification workflow for metaproteomic studies. *Brief Bioinform* 2019; doi:10.1093/bib/bby127.
- Li S, Li J, Ning L, et al. In silico identification of protein S-palmitoylation sites and their involvement in human inherited disease. *J Chem Inf Model* 2015;**55**:2015–25.
- Ashburner M, Ball CA, Blake JA, et al. Gene ontology: tool for the unification of biology. The gene ontology consortium. *Nat Genet* 2000;**25**:25–9.
- Clark WT, Radivojac P. Analysis of protein function and its prediction from amino acid sequence. *Proteins* 2011;**79**:2086–96.
- Frasca M, Cesa-Bianchi N. Multitask protein function prediction through task dissimilarity. *IEEE/ACM Trans Comput Biol Bioinform* 2017; doi:10.1109/TCBB.2017.2684127.
- Cao R, Cheng J. Integrated protein function prediction by mining function associations, sequences, and protein-protein and gene-gene interaction networks. *Methods* 2016;**93**:84–91.
- Schnoes AM, Ream DC, Thorman AW, et al. Biases in the experimental annotations of protein function and their effect on our understanding of protein function space. *PLoS Comput Biol* 2013;**9**:e1003063.
- Li YH, Yu CY, Li XX, et al. Therapeutic target database update 2018: enriched resource for facilitating bench-to-clinic research of targeted therapeutics. *Nucleic Acids Res* 2018;**46**:D1121–7.
- Yang H, Qin C, Li YH, et al. Therapeutic target database update 2016: enriched resource for bench to clinical drug target and targeted pathway information. *Nucleic Acids Res* 2016;**44**:D1069–74.
- Zhu F, Shi Z, Qin C, et al. Therapeutic target database update 2012: a resource for facilitating target-oriented drug discovery. *Nucleic Acids Res* 2012;**40**:D1128–36.
- Zhu F, Han B, Kumar P, et al. Update of TTD: therapeutic target database. *Nucleic Acids Res* 2010;**38**:D787–91.
- Cao R, Freitas C, Chan L, et al. ProLanGO: protein function prediction using neural machine translation based on a recurrent neural network. *Molecules* 2017;**22**:1732.

33. Zhu F, Han L, Zheng C, et al. What are next generation innovative therapeutic targets? Clues from genetic, structural, physicochemical, and systems profiles of successful targets. *J Pharmacol Exp Ther* 2009;**330**:304–15.
34. Xu J, Wang P, Yang H, et al. Comparison of FDA approved kinase targets to clinical trial ones: insights from their system profiles and drug-target interaction networks. *Biomed Res Int* 2016;**2016**:2509385.
35. Fu J, Tang J, Wang Y, et al. Discovery of the consistently well-performed analysis chain for SWATH-MS based pharmacoproteomic quantification. *Front Pharmacol* 2018;**9**:681.
36. Zhu F, Li XX, Yang SY, et al. Clinical success of drug targets prospectively predicted by *in silico* study. *Trends Pharmacol Sci* 2018;**39**:229–31.
37. Xue W, Yang F, Wang P, et al. What contributes to serotonin-norepinephrine reuptake inhibitors' dual-targeting mechanism? The key role of transmembrane domain 6 in human serotonin and norepinephrine transporters revealed by molecular dynamics simulation. *ACS Chem Neurosci* 2018;**9**:1128–40.
38. Jain A, Kihara D. Phylo-PFP: improved automated protein function prediction using phylogenetic distance of distantly related sequences. *Bioinformatics* 2019;**35**:753–9.
39. Zhang C, Freddolino PL, Zhang Y. COFACTOR: improved protein function prediction by combining structure, sequence and protein-protein interaction information. *Nucleic Acids Res* 2017;**45**:W291–9.
40. Wan S, Duan Y, Zou Q. HPSLPred: an ensemble multi-label classifier for human protein subcellular location prediction with imbalanced source. *Proteomics* 2017;**17**:1700262.
41. Cruz LM, Trefflich S, Weiss VA, et al. Protein function prediction. *Methods Mol Biol* 1654;**2017**:55–75.
42. Piovesan D, Giollo M, Ferrari C, et al. Protein function prediction using guilty by association from interaction networks. *Amino Acids* 2015;**47**:2583–92.
43. Lv Q, Ma W, Liu H, et al. Genome-wide protein-protein interactions and protein function exploration in cyanobacteria. *Sci Rep* 2015;**5**:15519.
44. Mateos A, Dopazo J, Jansen R, et al. Systematic learning of gene functional classes from DNA array expression data by using multilayer perceptions. *Genome Res* 2002;**12**:1703–15.
45. Huttenhower C, Hibbs M, Myers C, et al. A scalable method for integration and functional analysis of multiple microarray datasets. *Bioinformatics* 2006;**22**:2890–7.
46. Hawkins T, Chitale M, Kihara D. New paradigm in protein function prediction for large scale omics analysis. *Mol Biosyst* 2008;**4**:223–31.
47. Tiwari AK, Srivastava R. A survey of computational intelligence techniques in protein function prediction. *Int J Proteomics* 2014;**2014**:845479.
48. Vazquez A, Flammini A, Maritan A, et al. Global protein function prediction from protein-protein interaction networks. *Nat Biotechnol* 2003;**21**:697–700.
49. Peng W, Wang J, Cai J, et al. Improving protein function prediction using domain and protein complexes in PPI networks. *BMC Syst Biol* 2014;**8**:35.
50. Nariai N, Kolaczyk ED, Kasif S. Probabilistic protein function prediction from heterogeneous genome-wide data. *PLoS One* 2007;**2**:e337.
51. Hwang H, Dey F, Petrey D, et al. Structure-based prediction of ligand-protein interactions on a genome-wide scale. *Proc Natl Acad Sci U S A* 2017;**114**:13685–90.
52. Sillitoe I, Lewis TE, Cuff A, et al. CATH: comprehensive structural and functional annotations for genome sequences. *Nucleic Acids Res* 2015;**43**:D376–81.
53. Lam SD, Dawson NL, Das S, et al. Gene3D: expanding the utility of domain assignments. *Nucleic Acids Res* 2016;**44**:D404–9.
54. Holm L, Rosenstrom P. Dali server: conservation mapping in 3D. *Nucleic Acids Res* 2010;**38**:W545–9.
55. Maghawry HA, Mostafa MG, Gharib TF. A new protein structure representation for efficient protein function prediction. *J Comput Biol* 2014;**21**:936–46.
56. Pearson WR. Protein function prediction: problems and pitfalls. *Curr Protoc Bioinformatics* 2015;**51**:4.12.1–8.
57. Yu CY, Li XX, Yang H, et al. Assessing the performances of protein function prediction algorithms from the perspectives of identification accuracy and false discovery rate. *Int J Mol Sci* 2018;**19**:183.
58. Camacho C, Coulouris G, Avagyan V, et al. BLAST+: architecture and applications. *BMC Bioinformatics* 2009;**10**:421.
59. Potter SC, Luciani A, Eddy SR, et al. HMMER web server: 2018 update. *Nucleic Acids Res* 2018;**46**:W200–4.
60. Zhao B, Wang J, Wu FX. Computational methods to predict protein functions from protein-protein interaction networks. *Curr Protein Pept Sci* 2017;**18**:1120–31.
61. Peled S, Leiderman O, Charar R, et al. De-novo protein function prediction using DNA binding and RNA binding proteins as a test case. *Nat Commun* 2016;**7**:13424.
62. Li YH, Xu JY, Tao L, et al. SVM-Prot 2016: a web-server for machine learning prediction of protein functional families from sequence irrespective of similarity. *PLoS One* 2016;**11**:e0155290.
63. Lan L, Djuric N, Guo Y, et al. MS-kNN: protein function prediction by integrating multiple data sources. *BMC Bioinformatics* 2013;**14**:S8.
64. Gonzalez-Camacho JM, Crossa J, Perez-Rodriguez P, et al. Genome-enabled prediction using probabilistic neural network classifiers. *BMC Genomics* 2016;**17**:208.
65. Khan ZU, Hayat M, Khan MA. Discrimination of acidic and alkaline enzyme using Chou's pseudo amino acid composition in conjunction with probabilistic neural network model. *J Theor Biol* 2015;**365**:197–203.
66. Hayat M, Khan A. Predicting membrane protein types by fusing composite protein sequence features into pseudo amino acid composition. *J Theor Biol* 2011;**271**:10–7.
67. Naveed M, Khan A. GPCR-MPredictor: multi-level prediction of G protein-coupled receptors using genetic ensemble. *Amino Acids* 2012;**42**:1809–23.
68. Nath N, Mitchell JB. Is EC class predictable from reaction mechanism? *BMC Bioinformatics* 2012;**13**:60.
69. Shen HB, Yang J, Chou KC. Fuzzy KNN for predicting membrane protein types from pseudo-amino acid composition. *J Theor Biol* 2006;**240**:9–13.
70. Xue W, Wang P, Tu G, et al. Computational identification of the binding mechanism of a triple reuptake inhibitor amitifadine for the treatment of major depressive disorder. *Phys Chem Chem Phys* 2018;**20**:6606–16.
71. Li H, Yap CW, Ung CY, et al. Machine learning approaches for predicting compounds that interact with therapeutic and ADMET related proteins. *J Pharm Sci* 2007;**96**:2838–60.
72. Hernandez C, Mella C, Navarro G, et al. Protein complex prediction via dense subgraphs and false positive analysis. *PLoS One* 2017;**12**:e0183460.

73. Brylinski M. Unleashing the power of meta-threading for evolution/structure-based function inference of proteins. *Front Genet* 2013;**4**:118.
74. Brandes N, Ofer D, Linial M. ASAP: a machine learning framework for local protein properties. *Database* 2016;**2016**:baw133.
75. Zheng G, Yang F, Fu T, et al. Computational characterization of the selective inhibition of human norepinephrine and serotonin transporters by an escitalopram scaffold. *Phys Chem Chem Phys* 2018;**20**:29513–27.
76. Wang P, Zhang X, Fu T, et al. Differentiating physicochemical properties between addictive and nonaddictive ADHD drugs revealed by molecular dynamics simulation studies. *ACS Chem Neurosci* 2017;**8**:1416–28.
77. Pearson WR, Li W, Lopez R. Query-seeded iterative sequence similarity searching improves selectivity 5-20-fold. *Nucleic Acids Res* 2017;**45**:e46.
78. Fokkens L, Botelho SM, Boekhorst J, et al. Enrichment of homologs in insignificant BLAST hits by co-complex network alignment. *BMC Bioinformatics* 2010;**11**:86.
79. Fujimoto MS, Suvorov A, Jensen NO, et al. Detecting false positive sequence homology: a machine learning approach. *BMC Bioinformatics* 2016;**17**:101.
80. Wei L, Zou Q. Recent progress in machine learning-based methods for protein fold recognition. *Int J Mol Sci* 2016;**17**:2118.
81. Zhang ZQ, Zhao Y, Liao XK, et al. Deep learning in omics: a survey and guideline. *Brief Funct Genomics* 2019;**18**:41–57.
82. Zou Q, Xing PW, Wei LY, et al. Gene2vec: gene subsequence embedding for prediction of mammalian N-6-methyladenosine sites from mRNA. *RNA* 2019;**25**:205–18.
83. Fa R, Cozzetto D, Wan C, et al. Predicting human protein function with multi-task deep neural networks. *PLoS One* 2018;**13**:e0198216.
84. Zeng NY, Zhang H, Song BY, et al. Facial expression recognition via learning deep sparse autoencoders. *Neurocomputing* 2018;**273**:643–9.
85. Min S, Lee B, Yoon S. Deep learning in bioinformatics. *Brief Bioinform* 2017;**18**:851–69.
86. Zou X, Wang G, Yu G. Protein function prediction using deep restricted Boltzmann machines. *Biomed Res Int* 2017;**2017**:1729301.
87. Seo S, Oh M, Park Y, et al. DeepFam: deep learning based alignment-free method for protein family modeling and prediction. *Bioinformatics* 2018;**34**:i254–62.
88. Zou Q, Wan S, Ju Y, et al. Pretata: predicting TATA binding proteins with novel features and dimensionality reduction strategy. *BMC Syst Biol* 2016;**10**:114.
89. The UniProt Consortium. UniProt: the universal protein knowledgebase. *Nucleic Acids Res* 2018;**46**:2699.
90. El-Gebali S, Mistry J, Bateman A, et al. The Pfam protein families database in 2019. *Nucleic Acids Res* 2019;**47**:D427–32.
91. Brusco MJ, Shireman E, Steinley D. A comparison of latent class, K-means, and K-median methods for clustering dichotomous data. *Psychol Methods* 2017;**22**:563–80.
92. Noble WS. What is a support vector machine? *Nat Biotechnol* 2006;**24**:1565–7.
93. Jiang Y, Kang J, Wang X. RRAM-based parallel computing architecture using k-nearest neighbor classification for pattern recognition. *Sci Rep* 2017;**7**:45233.
94. Basant N, Gupta S, Singh KP. Predicting the acute neurotoxicity of diverse organic solvents using probabilistic neural networks based QSTR modeling approaches. *Neurotoxicology* 2016;**53**:45–52.
95. Han LY, Cai CZ, Ji ZL, et al. Predicting functional family of novel enzymes irrespective of sequence similarity: a statistical learning approach. *Nucleic Acids Res* 2004;**32**:6437–44.
96. Karchin R, Karplus K, Haussler D. Classifying G-protein coupled receptors with support vector machines. *Bioinformatics* 2002;**18**:147–59.
97. Dobson PD, Doig AJ. Distinguishing enzyme structures from non-enzymes without alignments. *J Mol Biol* 2003;**330**:771–83.
98. Bock JR, Gough DA. Predicting protein-protein interactions from primary structure. *Bioinformatics* 2001;**17**:455–60.
99. Eckle K, Schmidt-Hieber J. A comparison of deep networks with ReLU activation function and linear spline-type methods. *Neural Netw* 2019;**110**:232–42.
100. Chen Y, Mai Y, Xiao J, et al. Improving the antinoise ability of DNNs via a bio-inspired noise adaptive activation function rand softplus. *Neural Comput* 2019;**31**:1215–33.
101. Hamm CA, Wang CJ, Savic LJ, et al. Deep learning for liver tumor diagnosis part I: development of a convolutional neural network classifier for multi-phasic MRI. *Eur Radiol* 2019;**29**:3338–47.
102. Kim J, Calhoun VD, Shim E, et al. Deep neural network with weight sparsity control and pre-training extracts hierarchical features and enhances classification performance: evidence from whole-brain resting-state functional connectivity patterns of schizophrenia. *Neuroimage* 2016;**124**:127–46.
103. Sato M, Horie K, Hara A, et al. Application of deep learning to the classification of images from colposcopy. *Oncol Lett* 2018;**15**:3518–23.
104. Wang J, Yang B, An Y, et al. Systematic analysis and prediction of type IV secreted effector proteins by machine learning approaches. *Brief Bioinform* 2017; doi:10.1093/bib/bbx164.
105. Cui X, Yang Q, Li B, et al. Assessing the effectiveness of direct data merging strategy in long-term and large-scale pharmacometabonomics. *Front Pharmacol* 2019;**10**:127.
106. Li XX, Yin J, Tang J, et al. Determining the balance between drug efficacy and safety by the network and biological system profile of its therapeutic target. *Front Pharmacol* 2018;**9**:1245.